Journal of the Iranian Chemical Society (2022) 19:4017–4033
https://doi.org/10.1007/s13738-022-02588-7

REVIEW

Removal of anti-inflammatory drugs using activated carbon from agro-industrial origin: current advances in kinetics, isotherms, and thermodynamic studies

Antonia Sandoval-González[1] · Irma Robles[2] · Carlos A. Pineda-Arellano[3] · Carolina Martínez-Sánchez[1]

Received: 10 December 2021 / Accepted: 8 May 2022 / Published online: 3 June 2022

Abstract
Nonsteroidal anti-inflammatory drugs (NSAIDs) are highly consumed around the world and consequently found as emerging pollutants in water; they are found in concentrations up to μg L^{-1} making their removal a priority. In this matter, adsorption is an efficient alternative for drug removal, so using activated carbon (AC) as an adsorbent is a highly explored subject. The current interest is to obtain AC from waste, for example, those of agro-industrial origin, reducing this way the overall costs of the process. Although information regarding the use of AC from agro-industrial origin in the removal of NSAIDs is limited, an exclusive compilation is required to understand the state of the art to date. This work aims to update information related to the adsorption of ibuprofen, diclofenac, and naproxen on agro-industrial AC, and it is focused on the period 2016–2021. It highlights the characteristics of agro-industrial AC responsible for efficient adsorption. Recent adsorption studies, including kinetics, isotherms, and thermodynamics, are analyzed and compared. Progress on removing NSAIDs from real wastewater is also presented and finally proposed adsorption mechanisms and costs related to these removal processes.

Keywords Activated carbon · Adsorption · Agro-industrial waste · Anti-inflammatory drugs · Emerging pollutants

Introduction

Emerging pollutants are compounds that are not currently regulated and have not been sufficiently studied. Their presence in the environment may cause harm to human and environmental health [1, 2]. When classifying emerging pollutants, pharmaceuticals are interesting since they reach wastewater by several routes such as those from pharmaceutical industry, hospitals, as well as those of agricultural, livestock, and municipal origin, as exemplified in Fig. 1. Furthermore, the COVID-19 pandemic only worsens this situation, since the consumption of various pharmaceuticals has increased. This scenario has negative effects on the environment, and up to today, there has not been enough research in this matter (COVID-19/increase in pharmaceuticals in wastewater) [3].

Antibiotics are among the most frequently drugs identified in wastewater, followed by analgesics, and nonsteroidal anti-inflammatory drugs (NSAIDs). This latter group is the most widely used around the world. For this reason, they are often found in water considered one of the top ten persistent pollutants [4]. The most commonly consumed anti-inflammatories are ibuprofen, diclofenac, and naproxen (Fig. 1) so their presence in wastewater is common. In Mexico, for example, the reported concentration of ibuprofen and diclofenac is around 6 μg L^{-1} both urban and rural wastewater effluents. These levels are known to be toxic [5]. Both the aforementioned pharmaceuticals, plus naproxen, were found at concentrations equal or above the action limit (1 μg L^{-1}) reported for environmental risk assessment [6].

Although the harmful effects that pharmaceuticals have on human health are not yet fully identified, it is known that some of the main ones correspond to alteration of

✉ Carolina Martínez-Sánchez
csanchez@cideteq.mx

[1] CONACYT-Centro de Investigación y Desarrollo Tecnológico en Electroquímica, CIDETEQ, 76703 Pedro Escobedo, Querétaro, México

[2] Centro de Investigación y Desarrollo Tecnológico en Electroquímica, CIDETEQ, 76703 Pedro Escobedo, Querétaro, México

[3] CONACYT-Centro de Investigaciones en Óptica, A.C., Unidad Aguascalientes, Prol. Constitución 607, Fracc. Reserva Loma Bonita, 20200 Aguascalientes, Aguascalientes, México

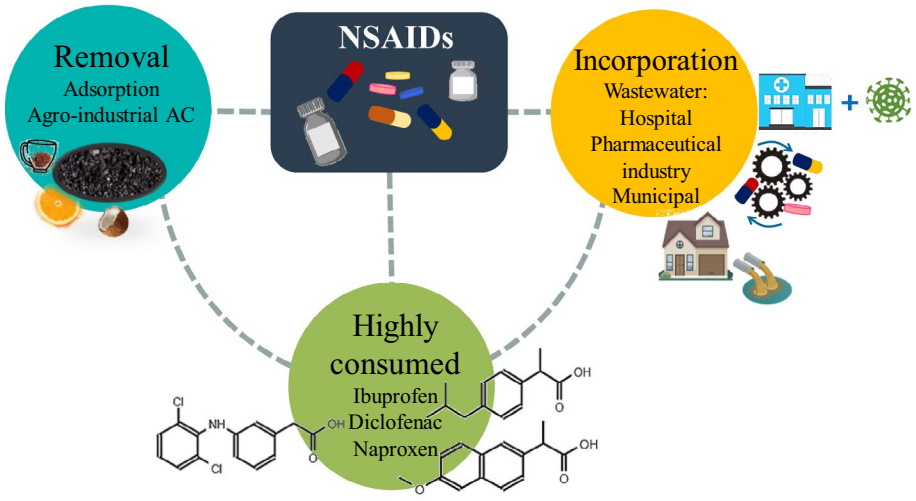

Fig. 1 Scheme of incorporation of the most frequently used NSAIDs to wastewater and their removal by agro-industrial AC

cellular processes and endocrine disruption [1]. Because of the impact of drugs on the environment and human health, their removal is a matter of interest. NSAIDs remain in the aqueous phase due to their hydrophilicity and stability, making their elimination difficult in traditional treatment plants [7]. For this reason, several methods have been studied, for example, biological treatments, advanced oxidation processes, and physicochemical treatments such as adsorption [8–10].

Adsorption is a simple method that satisfies the removal of various contaminants [7, 11, 12]. During the adsorption process, pollutants are captured from an aqueous solution by a material called adsorbent through physicochemical mechanisms. Using activated carbon (AC) as an adsorbent is recognized by the United States Environmental Protection Agency (USEPA) as an efficient technology for the removal of organic and inorganic compounds from water [13]. The interest nowadays is obtaining AC from different wastes, thus reducing the costs of this type of process, which gives meaning of agro-industrial origin AC. In this regard, there are many reviews analyzing the adsorption of pharmaceuticals (including anti-inflammatories) on AC obtained from different wastes [7, 14, 15]. However, there is little information on studies completely focused on AC from agro-industrial origin. There is current need of precise information describing the analysis and methods employed that allow the understanding of adsorption processes of NSAIDs on this type of AC. This paper aims to update the information reported in the last six years (2016–2021) on the adsorption of ibuprofen, diclofenac, and naproxen on agro-industrial AC, as well as the advantages of using agro-industrial waste and the key characteristics of the materials employed to obtain AC. Subsequently, the basic studies of adsorption that include kinetics, isotherms, and thermodynamics are analyzed, as well as the evaluation in the removal of NSAIDs in real wastewater, adsorption mechanisms, and costs associated with this type of process in order to determine viability towards implementation.

Activated carbon obtained from agro-industrial residues

The remaining biomass of a processed crop or agro-industrial processing is mainly composed of tissues that are part of the plant cell structure. The cell wall is mainly composed of cellulose, hemicelluloses, and lignin, and the fraction of these compounds varies depending on species, age, growing season, or industrial exploitation. Nieto compared biopolymers and the carbon composition of different organic wastes. For example, coconut shell, peach stone, and apricot stone contain the highest amount of carbon, around 50%, while an amount of cellulose of up to 45% has been identified in eucalyptus wood, agave bagasse, and beech wood. On the other hand, beech wood and apricot stone have hemicellulose of up to 30%; finally, the waste materials that contain the highest amount of lignin (up to 52%) are palm shell and walnut shell [16].

The cell wall of a plant is composed of different layers: the primary wall, the secondary wall, and the middle lamella. They all differ by their chemical composition. The primary cell wall is mainly comprised of cellulose, unbranched polymers composed of D-glucose molecules associated with the formation of cellulose crystallites. Pectin has a similar function to hemicelluloses since it also acts as a binder between cellulose microfibrils in the primary cell wall. Pectin is a complex mixture of polysaccharides provided with carboxylic groups, which are normally dissociated and have a negative charge, giving an ionic exchange capacity to the cell wall. The secondary cell wall is between

the plasma membrane and the primary cell wall, it incorporates lignin to its chemical composition, which is a phenolic macromolecule with a variable chemical structure. In the secondary cell wall, the cellulose microfibrils and hemicelluloses chains form a complex mixture of lignin, generating a rigid and tighter structure. Three different layers are then identified in the secondary cell wall since cellulose and hemicellulose appear to be more structurally organized [17]. These properties of organic waste, besides to the large volume generated worldwide, make biomass a material suitable for processing into activated carbon. For this purpose, the origin of the precursor and the method employed to convert it into AC can offer specific characteristics to the AC. The most frequently used methods to produce activated carbon from lignocellulosic materials are chemical, thermal, hydrothermal, and microwave-assisted activation. It is possible to produce a large number of activated carbon for different applications only by controlling the activation process [18].

Physical activation, also known as thermal activation, comprises the carbonization of the raw material under an inert atmosphere, followed by activation at a higher temperature under oxidizing gases. The carbon precursor develops porosity, and expanded surface area under these conditions. This process applies to lignocellulosic materials and mineral carbons. However, the preferred materials are high-rank carbons such as wood and lignocellulosic materials.

The chemical activation process involves carbonization and activation simultaneously using an activator agent promoting the formation of surface chemical groups. Cellulose degradation occurs between 240 and 350 °C, giving char and volatiles as the primary products [19]. Hemicelluloses are the most labile of the three basic biopolymers, it may decompose at temperatures between 180 and 260 °C, generating large amounts of volatiles and fewer char than cellulose. Finally, lignin decomposes between 280 and 500 °C. The pyrolysis of this fraction generates phenols via the cleavage of ether and carbon–carbon linkages. Lignin is the highest contribution of char since it is more difficult to dehydrate than cellulose or hemicellulose [20, 21].

Hydrothermal carbonization involves heating a mixture of water with organic substances between 150 and 350 °C under autogenous pressure conditions, it is also known as wet pyrolysis. Under hydrothermal carbonization, it is possible to decompose lignocellulosic materials in water-soluble organic substances and a carbon-rich solid product commonly named activated hydrochar [22–25].

Finally, microwave-assisted activation has been defined as the application of microwave heating for the activation of lignocellulosic materials. Microwave radiation provides energy to the entire structure of the material, turning the microwave radiation into heat inside the particles by dipole rotation and ionic conduction [26, 27]. Table 1 shows some literature reports on the synthesis of agro-industrial AC.

Activated carbon is an effective way to remove a wide range of contaminants from water. Many of the organic contaminants have chemical complex structures as aromatic rings with oxygen-containing substituents, including endocrine-disrupting compounds, pharmaceuticals, and personal care products, volatile organic compounds, halogenated organic compounds, and oxyanions. The focus of this review is on the NSAIDs ibuprofen, diclofenac and naproxen.

Adsorption process

Adsorption kinetics

According to Ho et al. [73] the adsorption process may be described in four successive stages: (1) transport in the solution, (2) diffusion through the boundary layer surrounding the adsorbent particles corresponding to an external diffusion, (3) intra-particle diffusion of the contaminant through the pores of the AC, and (4) adsorption of the pollutant into the pores through interaction with the functional groups until equilibrium is reached.

Diffusion rates are dictated by the molecular size relative to the pore width, specific molecule–wall interactions, pore tortuosity, molecular charge, surface charge, and water association [74].

This shows that equilibrium is not reached instantly and depends on the mass transfer of the pharmaceuticals into the pores. One of the previous steps or combinations can be the factors that control the rate of adsorption. To study the adsorption kinetics and determine the order of reaction are different mathematical models. The most studied models for adsorption of NSAIDs on AC are: intra-particle diffusion model, pseudo-first-order model, and pseudo-second-order model.

Intra-particle diffusion model

In 1964, Weber and Morris [75, 76] proposed the intra-particle diffusion model, where the graph of the adsorbed pollutant (q) as a function of the square root of the contact time must have a linear behavior according to Eq. (1). This shows that the limiting step is intra-particle diffusion.

$$q_t = k_p t^{0.5} + C \tag{1}$$

where q is the amount of pollutant adsorbed (mg g^{-1}), k_p is the intra-particle diffusion constant (mg g^{-1} $min^{-0.5}$), and C is the boundary layer thickness constant. However, it has been found that in several studies multi-linearity is present, which implies that two or more stages of the adsorption process are performed [77]. For example, Fig. 2 represents the process of pollutant interaction with AC and for

Table 1 Comparison of experimental conditions for the synthesis of activated carbon from agro-industrial waste

Precursor material	Experimental conditions	Surface area ($m^2\ g^{-1}$)	Sorption capacity (mg g^{-1})	References
Thermo-chemical activation				
Orange peel	H_3PO_4 [85%]; 400-800 ºC; 0.5–1 h; air	–	149 (Methylene blue)	[28]
Orange peel	H_3PO_4; 400 ºC; 0.5 h; air	470	410 (Methylene blue)	[29]
Jackfruit shell	H_3PO_4; 350–550 ºC; 0.5 h; N_2	1000–1200	–	[30]
Orange peel	H_3PO_4 [50%]; 475 ºC; 0.5 h; air	1090	320 (Methylene blue) 522 (Rhodamine B)	[31]
Used coffee ground	H_3PO_4 [2–20 mM]; 450 ºC; 2 h	514—925	–	[32]
Used coffee ground	H_3PO_4 [0–0.4 M]; 700 ºC; 1 h	76–147	–	[33]
Used coffee ground	H_3PO_4 [3–10 mM]; 450 ºC; 1 h	610–1003	–	[34]
Used coffee ground	H_3PO_4 [3–20 mM]; 450 ºC; 1 h	799–1402	–	[35]
Used coffee ground	H_3PO_4 [1:1]; 450 ºC; 1 h; N_2	–	29 (Methyl orange)	[36]
Orange peel	H_3PO_4 [40%]; 450 ºC; 3 h; N_2	451	122.3 (Phenol)	[37]
Orange peel	H_3PO_4; 600 ºC; 1 h; N_2	–	–	[38]
Orange peel	H_2SO_4 [98%]; 150 ºC; 12 h; air	–	33.8 (Direct blue-86)	[39]
Orange peel	H_2SO_4 [98%]; 120 ºC; 24 h; air	–	33.8 (Direct blue-106)	[40]
Orange peel	H_2SO_4 [98%]; 180 ºC; 2 h; air	–	75.8 (Direct yellow-12)	[41]
Orange peel	H_3PO_4 [0.6 M]; 400 ºC; 1 h; N_2	0.404	2343 (Methyl orange)	[38]
Olive stones	H_2SO_4 [10%]; 550 ºC; 1 h; air	–	8.7 (Diclofenac)	[42]
Cocoa pods	H_2SO_4 [98%]; 120 ºC; 24 h	–	5.53(Diclofenac)	[43]
Tea waste	H_2SO_4, KOH, $ZnCl_2$, K_2CO_3 [1:1] 600 ºC; 2 h	115–865	62 (Diclofenac)	[44]
Acorns	H_2SO_4, NaOH, KOH, NH_4Cl_2, $ZnCl_2$, H_3PO_4, 700–900 ºC; 1 h	234	45.45 (Acetaminophen) 96.15 (Ibuprofen)	[45]
Orange peel	HCl [-]; 500 ºC; 2 h; N_2	754	Iron	[46]
Orange peel	HCl [1 N]; 300 ºC; 1 h; N_2	–	983 (Iodine)	[47]
Astragalus Mongholicus wood	HCl [1 N]; 600 ºC; 1 h; N_2	156	59 (Diclofenac)	[48]
Used coffee ground	KOH [7–30 mM]; 750 ºC; 1 h	2290–2520	–	[49]
Orange peel	KOH [1 M]; 800 ºC; 2.5 h; N_2	1892	680 (Methyl orange)	[28]
Orange peel	KOH [60%]; 550 ºC; 4 h; Ar	897	40–69 (Cd, Cr, Co)	[50]
Pomelo peel	KOH; 450–800 ºC; 1.5–2.5 h; N_2	1892.1	680 (Methyl orange)	[29]
Date palm leaflets	KOH [0.1 M, 1:3]; 500 ºC; 2 h; N_2	9–823	65–454 (Chlorpheniramine) 23–73 (Ibuprofen)	[51]
Rice shell	NaOH; 650 ºC; 1 h; N_2	253	0.17 (Zn II)	[52]
Potato peel	K_2CO_3; [1:1]; 700 ºC; 0.1 h	866	146 (Diclofenac)	[53]
Used coffee ground	$ZnCl_2$[4–10 mM]; 800 ºC; 1 h	645–1121	–	[54]
Sugar cane bagasse	$ZnCl_2$[1:3]; 500 ºC; 2 h	1145	98 (Diclofenac)	[55]
Used coffee ground	$ZnCl_2$[18–73 mM]; 600 ºC; 1 h	550–900	–	[56]
Used coffee ground	$ZnCl_2$[0–7 mM]; 550 ºC; 3 h	965–1522	–	[57]
Used coffee ground	$ZnCl_2$[0–7 mM]; 500 ºC; 1 h	1450	–	[58]
Lovegrass	$ZnCl_2$[1:1]; 700 ºC; 1 h	1040	221(Cetylsalicylic acid) 312 (Diclofenac)	[59]
Avocado seed	$ZnCl_2$[1:1]; 500–700 ºC; 0.5–1 h; N_2	1122–1584	70–325 (amoxicillin, caffeine, captopril, meloxicam)	[60]
Banana peel	$ZnCl_2$; 1000 ºC; 8 h; N_2	1650	–	[61]
Thermo-physical activation				
Almond shell	CO_2; 300–1200 ºC; 1 h; N_2	320–385	289 (2-Picoline)	[62]
Orange peel	CO_2; 400–1200 °C; 1 h; N_2	220–250	167 (2-Picoline)	[62]
Pine white wood	400 °C; 2 h; N_2	1894	3.99 (Methylene blue)	[63]
Chili seeds	450–600 ºC; 2 h; N_2	0.52–0.18	4.5–11 (Ibuprofen)	[64]
Date stone seeds	700 ºC; 1 h; N_2	342–513	12.2 (Ibuprofen)	[65]

Table 1 (continued)

Precursor material	Experimental conditions	Surface area ($m^2\ g^{-1}$)	Sorption capacity (mg g^{-1})	References
Hydrothermal activation				
Olive waste	180 ºC; 4 h	–	–	[66]
Cornstalk	200 ºC; 0.45 h	–	(Cr (VI))	[67]
Tea stalk	313 ºC; 4 h	666.7	–	[68]
Apricot seed	323 ºC; 4 h	583.2	–	[68]
Microwave activation				
Corncob	KOH, 600 W, 4 h	1405	637 (Methylene blue)	[69]
Barley husk	H_3PO_4, 200 W, 4 min, N_2	–	103 (Methylene blue)	[70]
Corncob	H_3PO_4, 200 W, 4 min, N_2	–	98 (Methylene blue)	
Agave leaves	H_3PO_4, 200 W, 4 min, N_2	–	89 (Methylene blue)	
Almond or Walnut shell	$ZnCl_2 + FeCl_3 + FeCl_2$, 200–1000 W, 15 min	1000	130 (Methylene blue)	[71]
Pumpkin seed shell	H_3PO_4, 500–600 W, 10 min, N_2	967	23.5 (Doxycycline hydrochloride)	[72]

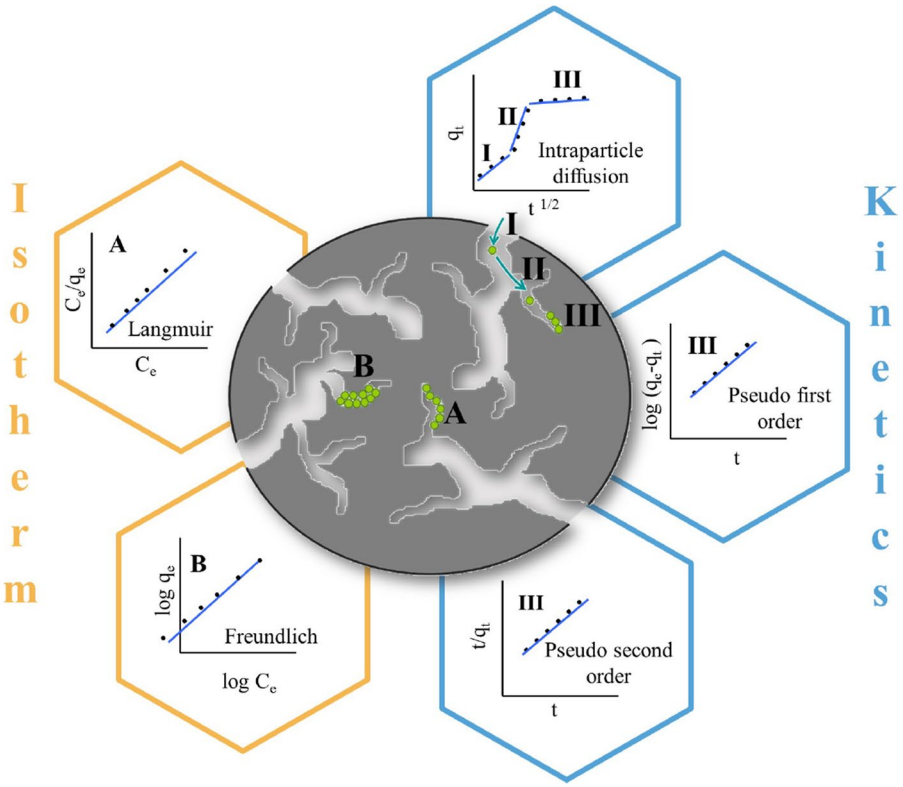

Fig. 2 Representation of the adsorption of NSAIDs on AC. I, II, and III correspond to external diffusion, intra-particle diffusion, and chemical interaction, respectively, and the kinetic models to which these stages are associated. A and B monolayer and multilayer adsorption, respectively, and related adsorption isotherms

intra-particle diffusion, three sections are observed in which the data are adjusted to three straight lines (I, II, and III). The first linear portion corresponds to external diffusion. The second corresponds to the intra-particle diffusion, which is the rate-limiting step. The third corresponds to the movement of the pollutant into the micropores, where it interacts with the active sites until reaching equilibrium. This interaction may be physical or chemical, so kinetic models need to be applied in order to predict the type of adsorption involved. The models employed correspond to pseudo-first order and pseudo-second order.

Pseudo-first-order model

The pseudo-first-order model was proposed by Lagergren in 1898 and is suitable to describe physical type adsorption, representing interactions that can be reversible (Fig. 2 III). The model assumes that the adsorption rate depends on the

difference between the instantaneous adsorption quantity and the saturated adsorption quantity [15] and is represented by Eq. (2) in its linearized form.

$$\ln(q_e - q_t) = \ln q_e - k_1 t \tag{2}$$

where k_1 (h^{-1}) is the pseudo-first-order rate constant, q_e and q_t (mg g^{-1}) are the adsorption capacity at equilibrium and at time t (h), respectively.

Pseudo-second-order model

This model was developed by Ho and Mckay in 1998 and originated from a chemical interaction between the metal ions and the active sites of the adsorbent, that is, chemisorption (Fig. 2 III) [73]. Assuming that the adsorption capacity is proportional to the number of active sites occupied in the adsorbent, the kinetic equation of the pseudo-second order model can be written in its linearized form as:

$$\frac{t}{q_t} = \frac{1}{kq_e^2} + \frac{1}{q_e} t \tag{3}$$

where k is the adsorption rate constant (g mg^{-1} min^{-1}), q_e is the amount of solute adsorbed at equilibrium (mg g^{-1}), and q_t is the amount of solute on the surface of the adsorbent at any time t (mg g^{-1}). The initial rate constant, h, can be determined from $h = kq_e^2$. The adjustment of the experimental data of this model shows that chemical interaction is the limiting step in the adsorption process.

Adsorption equilibrium

Equilibrium analysis of experimental data determines the capacity of the AC to adsorb pharmaceuticals from a solution, as well as constants that express the affinity between adsorbate and adsorbent [78]. The ratio of the adsorption equilibrium at any given temperature is called adsorption isotherm. The analysis of equilibrium data adjusted to the different isothermal models is of particular interest because they can be useful for the design and projection of the treatment at scale. Langmuir and Freundlich are the most frequently used isotherm models to describe adsorption of NSAIDs on AC.

Langmuir isotherm

The Langmuir model assumes that: (1) there is a finite number of active sites distributed homogeneously over the surface of the adsorbent, (2) the adsorption energy of all active sites is equal, and (3) only one molecule can be adsorbed at each site [79]. According to this model, pharmaceuticals interact with active sites until all of them are occupied, resulting in the formation of a monolayer, so equilibrium is reached (Fig. 2A). Langmuir's equation can be expressed as:

$$\frac{C_e}{q_e} = \frac{1}{k_L q_{\max}} + \frac{C_e}{q_{\max}} \tag{4}$$

where q_e is the amount of pharmaceutical adsorbed at equilibrium (mg g^{-1}), C_e is the concentration of the pharmaceutical in the solution (mg L^{-1}), $q_{\max}$ is the maximum adsorption capacity of the adsorbent can reach (mg g^{-1}), and k_L is the constant related to the binding affinity that the sites have (L mg^{-1}) for the pharmaceutical study.

Freundlich isotherm

The Freundlich isotherm is based on the heterogeneous surface of the AC, so all active sites have different energies, meaning that active sites with greater affinity or energy are first occupied with a higher bonding force. Later, the lower energy sites will be occupied, forming multilayers of adsorbed pharmaceuticals (Fig. 2B) [15]. Equation (5) represents Freundlich's model:

$$\log q_e = \log k_F + \frac{1}{n} \log C_e \tag{5}$$

where q_e is the amount of pharmaceutical adsorbed at equilibrium, C_e is the concentration of the pharmaceutical in the solution, and k_F and n are the Freundlich constants related to the adsorption capacity and intensity, respectively [80]. If the value of n is between 2 and 10 it is considered that the adsorption is good, if this value ranges between 1 and 2 the adsorption is moderately difficult, finally if the value of n is less than 1 the adsorption is poor [79].

Advanced adsorption models: statistical physics models

Although the Langmuir and Freundlich models are widely used, they are limited in the details of adsorption mechanisms by their theoretical knowledge. For this reason, the analysis and modelling of pharmaceutical adsorption using models based on statistical physics are now available, allowing interpretations of adsorption mechanisms at a molecular level [81]. Table 2 shows the proposed models that were developed by applying the grand canonical ensemble in statistical physics.

The parameter n describes the chemical behavior of pharmaceutical products in solution by estimating the aggregation of adsorption on AC. It also provides important information on the binding position of pharmaceutical

Table 2 Advanced adsorption models developed from statistical physics theory [81]

Model	Equation	Description
Monolayer model with single energy (M1)	$Q_e = \frac{nD_m}{1+\left(\frac{C_{1/2}}{C}\right)^n}$ n = number of pharmaceutical molecules captured by an AC active site D_m = adsorbent receptor site density $C_{1/2}$ = concentration at half-saturation	Assumes that adsorption of the pharmaceutical is by the formation of an adsorbed layer with a single energy. Each receptor site that contributes to adsorption can capture a variable number of pharmaceuticals defined by the parameter n
Monolayer model with two energies (M2)	$Q_e = \frac{n_1 D_{m1}}{1+\left(\frac{C_1}{C}\right)^{n1}} + \frac{n_2 D_{m2}}{1+\left(\frac{C_2}{C}\right)^{n2}}$ D_{m1} = receptor site density of the first type D_{m2} = receptor site density of the second type C_1 = half-saturation concentration of the first receptor site C_2 = half-saturating concentration of the second receptor site	It assumes the possibility that the pharmaceutical can be adsorbed at two different sites on the AC and each site can capture a variable number of pharmaceuticals identified as n_1 and n_2. Thus, the pharmaceutical is adsorbed with two different adsorption energies
Double layer model with two energies (M3)	$Q_e = nD_m \frac{\left(\frac{C}{C_1}\right)^n + 2\left(\frac{C}{C_2}\right)^{2n}}{1+\left(\frac{C}{C_1}\right)^n + \left(\frac{C}{C_2}\right)^{2n}}$ C_1 = half-saturation concentration of the first layer C_2 = half-saturation concentration of second layer	It assumes that adsorption can occur by forming two adsorbed layers. In addition to the double layer, the model assumes two interaction energies
Multilayer model with saturation (M4)	$Q_e = nD_m \frac{\frac{-2\left(\frac{C}{C_1}\right)^{2n}}{1-\left(\frac{C}{C_1}\right)^n} + \frac{\left(\frac{C}{C_1}\right)^n\left(1-\left(\frac{C}{C_1}\right)^{2n}\right)}{\left(1-\left(\frac{C}{C_1}\right)^n\right)^2} + \frac{2\left(\frac{C}{C_1}\right)^n\left(\frac{C}{C_2}\right)^n\left(1-\left(\frac{C}{C_2}\right)^{nN_2}\right)}{\left(1-\left(\frac{C}{C_2}\right)^n\right)} + \frac{N_2\left(\frac{C}{C_1}\right)^n\left(\frac{C}{C_2}\right)^n\left(\frac{C}{C_2}\right)^{nN_2}}{\left(1-\left(\frac{C}{C_2}\right)^n\right)} + \frac{\left(\frac{C}{C_1}\right)^n\left(\frac{C}{C_2}\right)^{2n}\left(1-\left(\frac{C}{C_2}\right)^{nN_2}\right)}{\left(1-\left(\frac{C}{C_2}\right)^n\right)^2}}{\frac{\left(1-\left(\frac{C}{C_1}\right)^{2n}\right)}{\left(1-\left(\frac{C}{C_1}\right)^n\right)} + \frac{\left(\frac{C}{C_1}\right)^n\left(\frac{C}{C_2}\right)^n\left(1-\left(\frac{C}{C_2}\right)^{nN_2}\right)}{\left(1-\left(\frac{C}{C_2}\right)^n\right)}}$ C_1 = half-saturation concentration of the first layer formed C_2 = half-saturation concentration of the other layers formed (N_2 layers). The total number of adsorbed layers is $N_c = 1 + N_2$	It assumes that pharmaceutical adsorption occurs by the formation of limited layers, which are. Adsorbate–adsorbent and adsorbate–adsorbate interactions are considered

molecules on the surfaces of materials during adsorption. From the analysis of the steric phenomenon (orientation of the pharmaceutical on the adsorbent surface), three cases can be analyzed: (1) $n \leq 0.5$, the molecule interacts with two or more sites at the AC surface and it is adsorbed in parallel orientation, this implies that adsorption can be performed by a multiple coupling process. (2) $0.5 < n < 1$, the molecule can be adsorbed on the AC by parallel and non-parallel orientation at the same time and (3) $n \geq 1$, the molecule can be adsorbed through a non-parallel orientation on the AC, in such a way that the adsorption is through a multimolecular process. In addition, when the value of n is close to 1, monomer formation is probable, 2 dimer formation and 3 trimer formation [82].

Thermodynamic study

Thermodynamic study shows how energy changes during the adsorption process [83]. The parameters determined are the change in the Gibbs energy, ΔG°, the change in enthalpy, ΔH°, and the change in entropy, ΔS°.

ΔG° indicates the spontaneity of a chemical reaction. Reactions occur spontaneously if at a certain temperature ΔG° is negative. The change in ΔG° is given by Eq. (6):

$$\Delta G^o = -RT \ln K \tag{6}$$

where R is the gas constant and K is the adsorption equilibrium constant and can be obtained from the relation between the amount adsorbed at equilibrium (q_e) and the equilibrium concentration (C_e).

The ΔH° indicates whether the reaction is exothermic or endothermic. The equilibrium constant can be expressed in terms of ΔH° as a function of temperature as follows:

$$\ln K = \frac{-\Delta H^o}{RT} + \frac{\Delta S^o}{R} \tag{7}$$

Equation (7) is known as the Van´t Hoff equation and ΔH° and ΔS° can be determined from the slope and the intercept of the graph of ln K as a function of 1/T. If the ΔH° has a value between 2.1 and 20.9 kJ mol^{-1} it is associated with a physisorption process, and if it is > 20 kJ mol^{-1}, it is associated with chemisorption [79].

Finally, a positive value of ΔS° indicates an increase in randomness at the adsorbent–solution interface during the adsorption process. This increase is associated with the adsorption of the pharmaceutical and the consequent release of water molecules that were originally bound, increasing the disorder of the system [79].

Current studies of the adsorption of ibuprofen, diclofenac, and naproxen on AC of agro-industrial origin

Table 3 shows the current studies that include the 2016–2021 period for the adsorption of diclofenac, ibuprofen, and naproxen on AC of agro-industrial origin. In addition, it can be seen that most of the studies (86% of the total reviewed) include a kinetic study. Reports analyzing the intra-particle diffusion model agree that adsorption of NSAIDs occurs in subsequent stages and that intra-particle diffusion depends on factors such as: (1) the hydrophilic nature of AC, the more hydrophilic nature, the greater wettability of the AC, reducing the boundary layer so the drug molecule dissolved in the aqueous medium is transferred more rapidly into the pores and (2) diameter and pore volume, since diffusion of the drug is difficult if the material has narrow pores [53].

On the other hand, adsorption of analyzed NSAIDs usually adjusts to a pseudo-second-order model suggesting that chemical interactions are the limiting step of the adsorption process, where k_2 is commonly in the order of 10^{-3} g mg^{-1} min^{-1}. For example, the adsorption of Diclofenac on AC obtained from different waste such as potato peel [53], sugarcane bagasse [55], soybean hulls [84], and cocoa pod husks [43] has similar values for k_2, but significant differences in the amount of pharmaceuticals adsorbed at equilibrium, q_e. Bernardo et al. [53] reported 74 mg g^{-1} adsorbed at equilibrium on AC-potato peel and $k_2 = 0.00125$ g mg^{-1} min^{-1}, while de Souza et al. [84] found that 19.42 mg g^{-1} was adsorbed at equilibrium on AC-Soybean hulls with $k_2 = 0.001$ g mg^{-1} min^{-1}. A similar value for k_2 means that the molecule interacts at the same rate with the AC functional groups, the only difference is the amount of adsorbed diclofenac, caused by differences in the surface area of different AC. For example, surface area for potato peel is 866 m^2 g^{-1} while 70 m^2 g^{-1} is found for Soybean hulls. Few studies report k_2 in the order of 10^{-2} g mg^{-1} min^{-1}, for example, a similar adsorption for naproxen on AC-Indian gooseberry seed shells [94] and ibuprofen on AC-Sludge from the beverage industry [90] can be attributed to their surface area (645 and 642 m^2 g^{-1}, respectively) compared to other studies shown in Table 3.

The adsorption equilibrium study is included in almost all recent studies of anti-inflammatories on agro-industrial AC, Table 3. Interestingly, in more than 60% of reports, all data adjust to a Langmuir model, meaning adsorption in a monolayer. When it comes to the adsorption of naproxen on two different materials, AC-Indian gooseberry seed shells [94] and AC-sugarcane bagasse [95], Langmuir's constant has the same order of magnitude of 0.15 and 0.23 L mg^{-1}, respectively, and so is the maximum adsorption capacity, q_{max}, 169 m^2 g^{-1} for AC-Indian gooseberry seed shells and

Table 3 Summary of research studies of adsorption of diclofenac, ibuprofen, and naproxen on AC-agro-industrial

Precursor	Isotherms models		Kinetic models		Thermodynamic parameters	References
	Langmuir	Freundlich	Pseudo-first order	Pseudo-second order		
Diclofenac						
Sugarcane bagasse	$k_L = 0.098$	$k_F = 89.220$	$k_1 = 0.260$	$k_2 = 0.009$	–	[55]
	$q_{max} = 315.000$	$n = 5.310$	$q_e = 50.600$	$q_e = 100.100$	–	
	$R^2 = 0.989$	$R^2 = 0.972$	$R^2 = 0.940$	$R^2 = 0.998$	–	
Olive stones	$k_L = 0.227$	$k_F = 2.266$	$k_1 = 0.010$	$k_2 = 1.159$	–	[42]
	$q_{max} = 11.00$	$n = 2.020$	$q_e = 1.064$	$q_e = 3.103$	–	
	$R^2 = 0.809$	$R^2 = 0.792$	$R^2 = 0.013$	$R^2 = 0.998$	–	
Potato peel	$k_L = 0.380$	$k_F = 33.400$	–	$k_2 = 0.001$	–	[53]
	$q_{max} = 68.50$	$n = 5.550$	–	$q_e = 74.000$	–	
	$R^2 = 0.931$	$R^2 = 0.916$	–	$R^2 = 0.852$	–	
Tea waste	$k_L = 0.576$	$k_F = 31.800$	$k_1 = 0.009$	$k_2 = 0.000155$	$\Delta H° = 6.950$	[44]
	$q_{max} = 91.20$	$n = 3.270$	$q_e = 63.500$	$q_e = 74.000$	$\Delta S° = 0.009$	
	$R^2 = 0.98$	$R^2 = 0.850$	$R^2 = 0.970$	$R^2 = 0.990$	$\Delta G° = -3.890$	
Soybean hulls	$k_L = 0.007$	$k_F = 4.230$	$k_1 = 0.027$	$k_2 = 0.001$	$\Delta H° = 20.913$	[84]
	$q_{max} = 122.920$	$n = 1.930$	$q_e = 17.540$	$q_e = 19.420$	$\Delta S° = 0.0002$	
	$R^2 = 0.959$	$R^2 = 0.881$	$R^2 = 0.993$	$R^2 = 0.982$	$\Delta G° = -20.967$	
Cocoa pod husks	$k_L = 1.869$	$k_F = 2.950$	$k_1 = 0.026$	$k_2 = 0.007$	–	[43]
	$q_{max} = 0.474$	$n = 4.340$	$q_e = 0.076$	$q_e = 5.672$	–	
	$R^2 = 0.980$	$R^2 = 0.997$	$R^2 = 0.382$	$R^2 = 0.999$	–	
Avocado seed	$k_L = -$	–	–	–	–	[60]
	$q_{max} = 132.00$	–	–	–	–	
	$R^2 = -$	–	–	–	–	
Peanut shell biomass -partially graphitic biochar	$k_L = 0.310$	$k_F = 58.600$	$k_1 = 1.159$	$k_2 = 0.015$	–	[85]
	$q_{max} = 128.30$	$n = 0.200$	$q_e = 97.0$	$q_e = 104.9$	–	
	$R^2 = 0.990$	$R^2 = 0.990$	$R^2 = 0.880$	$R^2 = 0.970$	–	
Fique bagasse	$k_L = 0.346$	$k_F = 20.000$	$k_1 = 0\ .002$	$k_2 = 9.24 \times 10^{-5}$	$\Delta H° = -82.110$	[86]
	$q_{max} = 57.100$	$n = 4.920$	$q_e = 9.690$	$q_e = 14.600$	$\Delta S° = -0.173$	
	$R^2 = 0.961$	$R^2 = 0.810$	$R^2 = 0.996$	$R^2 = 0.903$	$\Delta G° = -31.370$	
Forestry Biomass	$k_L = 0.250$	$k_F = 41.11$	$k_1 = 1.17$	$k_2 = 0.015$	$\Delta H° = 1.562$	[87]
	$q_{max} = 159.700$	$n = 0.440$	$q_e = 105.4$	$q_e = 112.\ 100$	$\Delta S° = 1.5 \times 10^{-5}$	
	$R^2 = 0.980$	$R^2 = 0.910$	$R^2 = 0.900$	$R^2 = 0.980$	$\Delta G° = -3.020$	
Ibuprofen						
Babassu coconut husk	$k_L = 0.320$	$k_F = 30.690$	–	–	–	[88]
	$q_{max} = 84.940$	$n = 3.816$	–	–	–	
	$R^2 = 0.962$	$R^2 = 0.996$	–	–	–	
Oak acorn	$k_L = 0.060$	$k_F = 7.743$	$k_1 = 0.015$	$k_2 = 0.001$	$\Delta H° = 24.850$	[45]
	$q_{max} = 96.150$	$n = 1.724$	$q_e = 21.990$	$q_e = 38.460$	$\Delta S° = 0.0805\ \Delta G° = 0.850$	
	$R^2 = 0.953$	$R^2 = 0.990$	$R^2 = 0.880$	$R^2 = 0.976$		
Babassu coconut	$k_L = 0.320$	$k_F = 30.700$	$k_1 = 0.202$	$k_2 = 0.004$	$\Delta H° = 19.200$	[89]
	$q_{max} = 84.900$	$n = 3.810$	$q_e = 79.600$	$q_e = 83.300$	$\Delta S° = 0.091$	
	$R^2 = 0.962$	$R^2 = 0.996$	$R^2 = 0.936$	$R^2 = 0.985$	$\Delta G° = -8.200$	
Chili seeds	$k_L = 0.012$	$k_F = 0.055$	–	–	–	[64]
	$q_{max} = 0.496$	$n = 3.060$	–	–	–	
	$R^2 = -$	$R^2 = -$	–	–	–	
Sludge from the beverage industry	$k_L = 0.234$	$k_F = 44.560$	$k_1 = 0.459$	$k_2 = 0.015$	–	[90]
	$q_{max} = 114.480$	$n = 1.850$	$q_e = 87.360$	$q_e = 89.530$	–	
	$R^2 = 0.991$	$R^2 = 0.949$	$R^2 = 0.991$	$R^2 = 0.998$	–	

Table 3 (continued)

Precursor	Isotherms models		Kinetic models		Thermodynamic parameters	References
	Langmuir	Freundlich	Pseudo-first order	Pseudo-second order		
Nauclea diderrichii seed epicarp	$k_L = 0.863$	$k_F = 0.204$	$k_1 = 0.024$	$k_2 = 0.011$	$\Delta H° = -30.320$	[91]
	$q_{max} = 70.920$	$n = 3.950$	$q_e = 43.660$	$q_e = 44.840$	$\Delta S° = 0.091$	
	$R^2 = 0.992$	$R^2 = 0.992$	$R^2 = 0.970$	$R^2 = 1.00$	$\Delta G° = -3.110$	
Peanut shell biomass -partially graphitic biochar	$k_L = 0.350$	$k_F = 25.900$	$k_1 = 1.138$	$k_2 = 0.027$	–	[85]
	$q_{max} = 66.300$	$n = 0.280$	$q_e = 50.700$	$q_e = 55.000$	–	
	$R^2 = 0.990$	$R^2 = 0.990$	$R^2 = 0.930$	$R^2 = 0.970$	–	
Rice straw-Based Biochar	–	–	$k_1 = 0.054$	$k_2 = 23.000$	–	[92]
	–	–	$q_e = 98.000$	$q_e = 165.000$	–	
	–	–	$R^2 = 0.920$	$R^2 = 0.990$	–	
Tamarind seed raw biochar	$k_L = 0.518$	$k_F = 4.590$	$k_1 = 1.143$	$k_2 = 0.080$	$\Delta H° = -113.510$	[93]
	$q_{max} = 10.570$	$n = 4.940$	$q_e = -$	$q_e = -$	$\Delta S° = -0.363$	
	$R^2 = 0.991$	$R^2 = 0.893$	$R^2 = 0.963$	$R^2 = 0.982$	$\Delta G° = -6.010$	
Naproxen						
Indian gooseberry seed shells	$k_L = 0.154$	$k_F = 38.480$	$k_1 = 0.550$	$k_2 = 0.013$	–	[94]
	$q_{max} = 169.490$	$n = 2.700$	$q_e = 88.870$	$q_e = 156.010$	–	
	$R^2 = 0.980$	$R^2 = 0.990$	$R^2 = 0.990$	$R^2 = 0.990$	–	
Sugarcane bagasse	$k_L = 0.231$	$k_F = 28.840$	$k_1 = 0.031$	$k_2 = 0.007$	$\Delta H° = -22.030$	[95]
	$q_{max} = 166.660$	$n = 2.040$	$q_e = 37.540$	$q_e = 38.020$	$\Delta S° = -0.0545$	
	$R^2 = 0.998$	$R^2 = 0.891$	$R^2 = 0.884$	$R^2 = 0.996$	$\Delta G° = -5.500$	
Peanut shells	$k_L = 0.009$	$k_F = 33.000$	$k_1 = 0.034$	$k_2 = 0.002$	$\Delta H° = -8.800$	[96]
	$q_{max} = 324.000$	$n = 0.330$	$q_e = 271.000$	$q_e = 304.000$	$\Delta S° = 0.004$	
	$R^2 = 0.986$	$R^2 = 0.975$	$R^2 = 0.964$	$R^2 = 0.957$	$\Delta G° = -20.300$	

Units of the parameters of models. Langmuir: k_L = L mg^{-1}; q_{max} = mg g^{-1}. Freundlich: k_F = ((mg g^{-1})(L mg^{-1})$^{1/n}$). Pseudo-first order: k_1 = min^{-1}; q_e = mg g^{-1}; Pseudo-second order: k_2 = g mg^{-1} min^{-1}; q_e = mg g^{-1}. Thermodynamic parameters: $\Delta H°$ = kJ mol^{-1}; $\Delta G°$ = kJ mol^{-1} @ 25 °C; $\Delta S°$ = kJ mol^{-1} K^{-1}

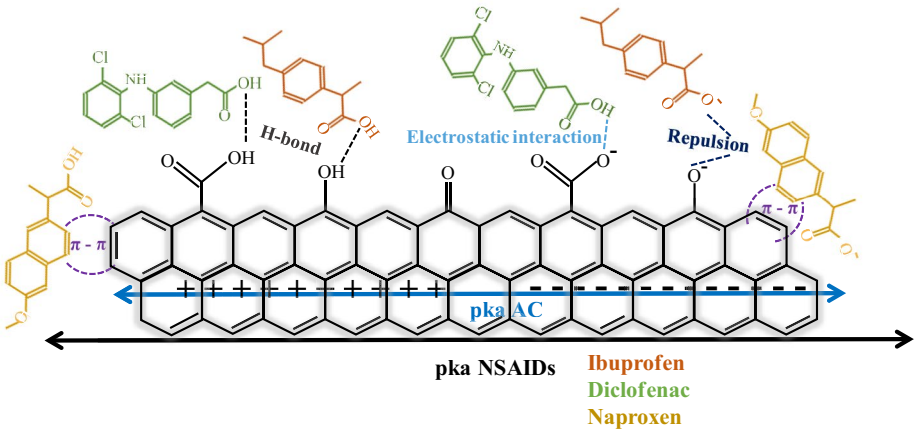

Fig. 3 Interactions between NSAIDs and AC that define the adsorption mechanism

166 m^2 g^{-1} for and AC-sugarcane bagasse. These results are attributed to a similar surface area between AC from Indian gooseberry seed shells and sugarcane bagasse (around 650 m^2 g^{-1}). Among all reports, the highest value of q_{max} corresponds to the adsorption of diclofenac on AC-sugarcane bagasse (315.00 mg g^{-1}), a material with the largest surface area (1145 m^2 g^{-1}). Some authors suggest that pore size is directly related to the adsorption capability. AC with a high number of mesoporous channels effectively connects the mesopores with the micropores, enhancing adsorption [86].

The adsorption affinity of NSAIDs on AC given by the k_L parameter varies from each report, indicating that affinity not only depends on the surface area, but it is also strongly related to the surface chemistry of the corresponding AC presented in Table 3. In this sense, the three main interactions between pollutants and AC functional groups are Van der Waals-type interactions, π-π interactive forces, and hydrogen bonding [96].

On the contrary, the adsorption of ibuprofen adjusts to the Freundlich model, thus it can be deduced that after forming a monolayer, there are subsequent physical interactions in order to form a multilayer. This can be attributed to a simpler structure (only one aromatic ring) and a lower molecular weight for ibuprofen [89] compared to naproxen and diclofenac (see structures in Fig. 3). This facilitates interactions with the AC and the formation of a multilayer. The value of n for the adsorption of the three NSAIDs ranges from 1.72 to 5.55, and therefore, it can be considered that in most studies the adsorption is efficient. n values are particularly high for diclofenac, reaching a value of 5.55 for adsorption on AC-Potato peel, indicating that diclofenac is the pharmaceutical with the best interaction with agro-industrial AC among all NSAIDs mentioned in this report.

It is important to mention that advanced statistical physics models have allowed a more detailed understanding of the adsorption process. For example, it has been determined that the calculated values of n (Equations in Table 2) were less than 1 for the adsorption of ibuprofen on AC from vegetal origin, demonstrating that the adsorbed ibuprofen molecule was shared by two or more sites with a parallel adsorption geometry [81]. The adsorption mechanism of diclofenac on cocoa shell-based adsorbents and plasma functionalized biomass involved a multimolecular process with a non-parallel orientation and no dimer formation [97]. This means that the physicochemical characteristics of the adsorbent surface are essential to determine the adsorption mechanism. Aggregation phenomena (drug-drug interactions before adsorption) are strongly influenced by temperature. In the case of diclofenac, the n value increased from 1.13 to 2.06 by increasing temperature, giving rise to dimer formation at 40 °C [98]. Similar behavior was presented for the adsorption of ibuprofen [82].

From these data, Langmuir and Freundlich models can be considered as an initial approximation for understanding the adsorption processes that can be complemented with advanced models that provide details on the anti-inflammatory adsorption process (a mechanism).

Finally, only 45% of the analyzed reports included a thermodynamic study. Most processes are spontaneous at room temperature according to the negative values of $\Delta G°$, since agro-industrial AC has several active sites available for adsorption. The more negative the value of $\Delta G°$, a better adsorption is observed for the material [86]. Diclofenac adsorption on Soybean hulls has a $\Delta G° = -20.967$ kJ mol^{-1} and $q_{max} = 122.92$ mg g^{-1} [84] while naproxen adsorption on Peanut shells has a $\Delta G° = -20.300$ and $q_{max} = 324.00$ mg g^{-1} [96]. Comparing these $\Delta G°$ values to the rest of the reports in Table 3, it can be determined that very negative values of $\Delta G°$ are indeed correlated with a higher q_{max} value.

The $\Delta H°$ values can be divided into three groups, the positive ones (endothermic) and less than 20 kJ mol^{-1}, suggesting a physisorption process. Those greater than 20 kJ mol^{-1}, between 20.9 and 24 kJ mol^{-1}, indicating chemisorption, and finally those with a negative value due to exothermic processes. It is noteworthy that $\Delta H°$ values less than 20 kJ mol^{-1} fit to a pseudo-first-order kinetics with $R^2 > 0.93$

Table 4 Summary of research studies of adsorption of diclofenac, ibuprofen, and naproxen on AC agro-industrial in wastewater

Precursor	Wastewater matrix	Adsorbed NSAIDs	Adsorption capacity (mg g^{-1})	Removal (%)	References
Sludge from the beverage industry	Simulated pharmaceutical effluent	Ibuprofen	105.91	85.16	[90]
Spent coffee wastes	Lake water	Diclofenac Ibuprofen Naproxen	28.76	55	[99]
			15.69	42	
			61.93	98	
	Municipal wastewater	Diclofenac Ibuprofen Naproxen	28.74	30	
			15.27	27	
			60.63	85	
Date palm leaflets	Spiked hospital wastewater	Ibuprofen	41.66	–	[51]
Coconut shell	Municipal wastewater	Diclofenac Ibuprofen Naproxen	–	98.95	[100]
			–	99.85	
			–	99.72	
Peanut shell biomass	Tap water	Diclofenac Ibuprofen	70.7	–	[85]
			14.3	–	

[44, 89] indicating that physical interactions are predominant in the adsorption process. Ahmed et al. [7] reported the adsorption of NSAIDs on AC obtained from different sources of waste with negative ΔH° values especially for ibuprofen. Table 3 suggests most processes are endothermic, indicating that adsorption can vary depending on the type of AC employed; observations are consistent with the report by Quesada et al. [14] on the adsorption of pharmaceuticals on low-cost materials. Finally, ΔS° positive values are reported in most studies, indicating increased randomness due to the adsorption effect of the pharmaceutical on AC.

According to all reports analyzed in this review, the frequency at which data is included follows the order equilibrium > kinetic > thermodynamics. It is recommended to perform a thermodynamic evaluation for the adsorption process since it can provide information on the effect of temperature. This allows the establishment of operating parameters to create strategies for the escalation of this type of water treatment.

Removal of NSAIDs from wastewater

In real wastewater, the adsorption capacity may vary compared to the adsorption of pollutants in solutions prepared in distilled or deionized water. In wastewater, pharmaceuticals are not found individually, and thus, the presence of other contaminants and inorganic salts may increase or inhibit the adsorption capacity. Table 4 shows recent reports where the adsorption of NSAIDs in wastewater from different sectors was evaluated. Ali et al. [51] reported the adsorption of ibuprofen on AC-Date palm leaflets in deionized water and enriched hospital wastewater; the experimental results were 52.4 and 41.66 mg g^{-1}, respectively; a decrease of about 20% in the amount of pharmaceutical adsorbed in real wastewater is observed. Hospital wastewater contains considerable amounts of dissolved organic matter, competing with ibuprofen for the active sites in the AC. Streit et al. [90] evaluated the adsorption of ibuprofen on AC-sludge from the beverage industry mixed with ketoprofen and paracetamol, simulating pharmaceutical industrial effluents. A removal of ibuprofen of 85% despite competition with other pharmaceuticals was observed, which can be attributed to the high surface area of the AC. Shin et al. [99] reported the adsorption of ibuprofen, diclofenac, and naproxen on AC-spent coffee waste in two different types of water, in lake water and wastewater effluents, finding similar adsorption capacities in both matrices. In both cases, the removal percentage are low for ibuprofen and diclofenac. Authors emphasize that high concentrations of Na^{+} increases ionic strength favoring removal and that π-π interactions between pharmaceuticals (aromatic rings) and AC play a fundamental role. NSAIDs adsorption on AC-coconut shell of secondary effluents from municipal wastewater under up-flow fixed bed reactors was carried out [100]. Removal percentage of 99% were reported in around five minutes of contact. Authors demonstrated that, when the adsorption process is coupled as a final treatment, for example, after peroxymonosulfate oxidation, the removal is greater, so this can be a practical application for post-treatment of urban wastewater effluents.

These studies show that the behavior can be different when transferring the studies to real wastewater, to date, few studies use real wastewater compared to those carried out in pure water. Although adsorption as a method for removing contaminants was studied a few years ago, its practical applications have not yet been studied in detail. To evaluate the feasibility of these types of removal systems, it is essential to include the assessment in real wastewater.

Adsorption mechanism

There are two ways in which the contaminant is adsorbed on the surface of the AC, physisorption, and chemisorption. Physisorption involves binding to the adsorbent surface by weak forces such as electrostatic attraction and Van der Waals forces, forming a multilayer. On the other hand, chemisorption is carried out through covalent bonds, coordination, and attraction of opposite or coulombic ions. This process is slow and can only form a monolayer on the surface of the adsorbent. The parameters that determine the type of interaction, whether physical or chemical, and therefore the adsorption mechanism [101–105] are surface area and pore size of the AC [106], nature of the adsorbate, initial pharmaceutical concentration (this parameter is important because it is the driving force [concentration gradient] for the mass transfer between the solution and the adsorbent), temperature, adsorbent dosage, contact time, competition between various solutes (as it occurs with adsorption in real contaminated water) and pH. The latter one is of special relevance since it influences the species distribution in which the pharmaceutical is found in solution, as well as the charge on the surface of the AC, as exemplified in Fig. 3.

Removing contaminants from water by carbonaceous porous materials involves the combination of adsorption mechanisms such as (a) pore filling, (b) formation of hydrogen bonds, (c) interactions n-π and π-π, (d) electrostatic attraction, and (e) Van der Waals forces, which are related to the chemical properties of the adsorbent surface [14, 15, 95, 107–109]. Disclosure of adsorption mechanisms is challenging. In recent years, they have been combined with the Fourier transform infrared spectroscopy analysis and the calculation of the density-functional theory (DFT), which has been widely applied to reveal adsorption mechanisms at the molecular level [107].

Diclofenac is a weak acid ($pK_a = 4.1$) and pH < 4.1 in its undissociated form. It is an ionizable compound. Diclofenac has functional groups such as chlorine, carboxylic acid, and two aromatic rings with strong electron capture capabilities. However, variation in pH affects adsorption through electrostatic attraction or repulsion. At pH 2 to 7, diclofenac can be easily adsorbed because of its positive charges, but at basic pH there is an electrostatic repulsion between the deprotonated carboxylic acid of the diclofenac and the negatively charged adsorbent surface, decreasing the adsorption capacity (Fig. 3). Abo El Naga et al. [55] reported that when a diclofenac solution had a pH less than 7, 97.4 mg g^{-1} was adsorbed on AC-bagasse from sugar cane. Adsorption at pH 7 decreases to 90 mg g^{-1} and pH 12 adsorption is sharply affected, decaying to 42 mg g^{-1}, which is in agreement with other authors since diclofenac is deprotonated and there are no electrostatic interactions between the adsorbent and adsorbate [55, 84, 110, 111]. The adsorption mechanism proposed is based on: (1) the H bonds between the functional groups of diclofenac and AC, considering AC as the donor of H to the phenolic ring (pH ~ 10) or the carboxylic acid (pH ~ 4.9); (2) π-π interactions between the donor and acceptor of electrons between the surface of the AC (π-electron donor) and the aromatic rings of the diclofenac (π electron acceptors) and (3) hydrophobic interactions between the adsorbent surface and adsorbed molecules [55]. These interactions may be related to the observed in adsorption isotherms where the diclofenac exhibits strong interaction with AC. On the other hand, Jung et al. [112], prepared an AC-pine chip under nitrogen (N) and oxygen (O) atmosphere for the adsorption of different pharmaceuticals. Among them, diclofenac showed maximum adsorption capacity of 372 and 214 mg g^{-1} for N-AC and O-AC, respectively. The adsorption mechanism was carried out by π-π interactions and between donor and electron acceptor between phenyl groups in diclofenac (electron acceptors) and the polarizable AC (electron donors). Viotti et al. [113] suggested that the adsorption mechanism of diclofenac is carried out through hydrogen bonds and π-π interactions between the aromatic ring of diclofenac and AC. In this scenario, most of the research indicates that electrostatic interactions and H bonds are the dominant mechanisms in the adsorption of diclofenac on AC [53, 106, 110, 111, 113–116]. With hydrogen bonds, the hydrogen donor is generally bonded to hydrogen acceptor atoms that can be functional groups of both, pharmaceutical and AC as well as –COOH, $-NH_2$, and –OH.

Naproxen is a molecule with a pK_a of 4.2, and two aromatic rings. The adsorption mechanism of naproxen on AC has been associated with an electron donor–acceptor π-π interaction and a high Van der Waals interactions between naphthalene (in naproxen) with AC [112]. Reynel-Avila et al. [104] propose that the adsorption mechanism of naproxen in bone char (carbon and calcium phosphate in the form hydroxyapatite) presents a complexation process through naproxen–phosphate interactions and hydrophobic interactions through π-π electron between the aromatic rings of naproxen and the aromatic rings of bone char (Fig. 3). DFT calculations reveal that the anionic ion of naproxen could be adsorbed through Lewis acid/base complexation and the anion-π interaction, in addition to the donor electron–acceptor π-π interaction and the binding of the hydrogen [107]. Moreover, the π-π interaction between phenol and nitrobenzene of the adsorbent (where the π-electrons act as donors) and the aromatic rings of naproxen (where the π-electrons act as acceptors) were considered. Infrared and Raman spectroscopy is used to confirm the H-bond and π-π interaction [95, 96].

Meanwhile, ibuprofen has a smaller molecular structure with only one aromatic ring, composed of hydrophilic and hydrophobic parts, it is dipolar and its pK_a is 4.91. Jung et al. [112] reported that the hydrophobicity of ibuprofen ($\log K_{ow} = 1.82$ at pH = 7) causes the binding energy through the benzene ring, allowing ibuprofen to be adsorbed on the pores of the AC occupying smaller sites of the exposed surface area of the AC, which explains the enhanced adsorption of ibuprofen compared to the other two. It also maximizes the π-π interactions between the surface of the AC and the solute, resulting in high binding energy. This is in agreement with the observed adsorption isotherms, where the ibuprofen may preferably be adsorbed in multilayers. Other researchers suggest that π-π interactions are the strongest in ibuprofen adsorption [107, 112]. Other authors indicate that one of the most likely mechanisms could be the interaction between methylene and amide functional groups of AC [15, 88]. A same as the other two reviewed NSAIDs, ibuprofen presents better adsorption at pH below 7. At neutral pH, the elimination of ibuprofen decreases, which may be because of a repulsive interaction between the negative charge of both drug and AC (Fig. 3) [113].

Finally, it is important to point out that a few of the reviewed papers include an adsorption mechanism proposal. The use of computational simulation tools is a suitable alternative for this analysis. Describing in detailed adsorption mechanisms is fundamental to understand whether modifications on the surface of the AC favor the adsorption of a certain pollutant, or how the chemical nature affects its selectivity, it can even be predicted the adsorption behavior in real residual water.

Cost–benefit analysis

The major disadvantages when using AC for widespread treatment of aqueous pollutants are its high cost and low availability. In this sense, one of the most important concerns is to reduce the production cost of the adsorbent compared to commercial AC (21 USD/Kg) [117]. Total sales of

AC around the world are estimated to be approximately 1 billion USD and 60% are manufactured from coal. On the other hand, the estimated production cost per kilogram of adsorbent prepared from agricultural residues is calculated around 4.5 USD, which represents approximately 1/4 the price of commercial AC and 1/20 the price of zeolite [118].

In order to carry out the adsorption process to treat contaminated wastewater, specifically pharmacological residues, interesting efforts have been made to reuse organic waste to manufacture efficient adsorbent materials, whether from agricultural waste, organic garbage, food-industry waste, or by-products of large organic process industries. Among these efforts, one of the most important is to reduce cost in the manufacture of adsorption materials without affecting the performance of the process, this contributes in two aspects; first, to partially recover and reuse organic waste, and second, to reduce environmental deterioration. In this way, it is desired to replace commercial materials based on inorganic carbon with environmentally friendly materials and at a reasonable cost [119]. However, in the literature, there are few reports where the production cost or the effectiveness of organic adsorbents are studied for the adsorption of NSAIDs.

There are few reports that focused specifically on the adsorption process to remove pollutants form the pharmaceutical industry. In this scenario, Nielsen and Bandosz [120]; reported the removal of sulfamethoxazole and trimethoprim by adsorption on a material obtained from pyrolyzed fish waste mixed with sewage-sludge. The overall cost of large-scale production of this material was 5 USD/Kg, which is highly competitive compared to the price of commercial AC. Authors evaluated different compositions of activated/pyrolyzed fish sludge at different temperatures, concluding that those treated at 950 °C composed of 90% sewage sludge and 10% fish waste had the best performance. They also highlighted the importance of surface chemistry as a favorable factor for eliminating pharmaceutical products in aqueous phase, as well and acid–base and polar interactions. Moreover, a recent theoretical study based on obtaining AC from the recovery of walnut-shell residues establishes an estimated production cost of 2.15 USD/Kg. This study was based on a plant capable of processing 31.25 Tons of walnut shells per day and producing 6.6 Tons of AC per day. To do this, several important input parameters were considered, such as the volume of raw material processing, the cost of the main equipment, the actual price of the walnut shell, and different tax rates with and without financing [121].

Grassi and coworkers reported the price of a series of adsorbents including some low-cost and environmentally friendly adsorbents such as sphagnum moss peat (0.02 USD/Kg), bagasse fly-ash (0.02 USD/Kg), fullers earth (0.1 USD/Kg), almond shell AC (2.2 USD/Kg) and chitosan (16 USD/Kg) [117]. An agro-industrial residue available in developing countries is rice husk, which has a high potential to be used as an adsorbent material because of its high content of carbon and silica, at a very competitive commercial price (~0.025 USD/kg) [122]. Another interesting work developed to increase an adsorbent capable of treating wastewater contaminated with pharmaceuticals (enrofloxacin) was carried out by Chowdhury et al. [123]. The AC was prepared from waste sludge from the paper industry, in which some important factors were considered such as the cost of raw material, the cost of drying the raw material, the cost per carbonization process, and washing (phosphoric acid)/drying costs, among others. The study showed a competitive cost of 207 INR (~2.82 USD) per Kg of AC derived from industrial paper sludge. An additional cost that was analyzed was the addition of orthophosphoric acid during the preparation of the adsorbent, in order to increase surface area and porosity. This report also showed a practical regeneration capacity.

One of the most important aspects to consider is the acquisition cost of the raw material and the treatment price. This aspect is not usually considered but is desirable. Chakraborty and his working group studied the adsorption capacity of ibuprofen in aqueous solution using apple-wood as an adsorbent, evaluating the performance of crude and steam AC [124]. Authors reported a 90% and 95% increase in maximum pollutant removal due to steam activation treatment, which represents production costs of 245.3 INR (3.35 USD) and 255.59 INR (3.49 USD) per Kg of biochar, respectively. In this study, although the differences between the preparation costs are not very representative, the most important impact was observed in the improvement of the regeneration capacity of the treated material and the absorption capacity after consecutive cycles. For these reasons, cost–benefit analysis must be carefully performed.

Conclusions

In this work, the current advances in the adsorption of ibuprofen, diclofenac, and naproxen on AC from agro-industrial origin were examined.

It has been observed that NSAIDs adsorption usually follows a pseudo-second-order model suggesting that chemical interactions are the limiting step in the adsorption process, where k_2 is generally in the order of 10^{-3} g mg^{-1} min^{-1}. Data from most of the analyzed papers regarding adsorption isotherms fit into the Langmuir model. However, application of advanced statistical physics models is important, from which the adsorption process is understood in detail. Interestingly, of the three pharmaceuticals analyzed in this review, diclofenac interacts strongly with agro-industrial AC. It is necessary to include thermodynamic studies since only a few reports

calculate ΔG°, ΔH°, and ΔS°, which change considerably depending on the surface chemistry of the AC.

Up to today, few studies employ real wastewater compared to those carried out in pure water, so the behavior observed in the experimental results can be very different when translating these methods to real wastewater. It is important to determine the adsorption capacity in actual waste water since this knowledge is fundamental when it comes to the development of adsorption methodologies potentially employed at grand scale. It is noteworthy that few of the reviewed literature includes a proposal for the adsorption mechanism. Removing NSAIDs from water using agro-industrial AC involves the combination of adsorption mechanisms such as pore filling, the formation of hydrogen bonds, the interactions *n*-π and π-π, electrostatic attraction, and Van der Waals forces. Current developments include the use of computer simulation combined with the results obtained by the Fourier transform infrared to reveal adsorption mechanisms.

Finally, it was found that cost information is currently limited. Some authors provide waste acquisition and AC preparation costs, which can be lower than commercial AC. However, this information is further limited to reports that also include operational costs and show the global cost–benefit of this type of pollutant removal process, which becomes a challenge to be addressed.

Acknowledgements The authors express their gratitude to the Mexican Council for Science and Technology, the Cátedras-CONACYT program, and the CB-2019-01-285309 project. The authors also thank the Center for Research and Technological Development in Electrochemistry for the facilities provided for the development of this work.

Author contributions ASG performed conceptualization, literature search, and data analysis, writing-original draft. IRG performed the literature search and data analysis, funding acquisition, and writing-original draft. CAPA performed writing-review and editing, and data analysis. CMS performed conceptualization, literature search, data analysis, and writing-original draft.

Funding This work was supported by the Mexican Council for Science and Technology, the Cátedras-CONACYT program, and the project CONACYT-Basic-Science [grant number CB-2019-01-285309].

Declarations

Conflict of interest The authors declare that they have no conflict of interest.

Data availability The authors confirm that the data supporting the review are available within the article (see "References" section).

Ethical approval Not applicable.

Consent to participate Not applicable.

Consent for publication Not applicable.

References

1. D. O'Flynn, J. Lawler, A. Yusuf, A. Parle-McDermott, D. Harold, T. Mc Cloughlin, L. Holland, F. Regan, B. White, Analyt. Methods **13**, 575 (2021)
2. M.C. Ncibi, B. Mahjoub, O. Mahjoub, M. Sillanpää, Clean: Soil, Air, Water (2017). https://doi.org/10.1002/clen.201700101
3. E.R. Bandala, B.R. Kruger, I. Cesarino, A.L. Leao, B. Wijesiri, A. Goonetilleke, Sci. Total Environ. **774**, 145586 (2021)
4. P. Izadi, P. Izadi, R. Salem, S.A. Papry, S. Magdouli, R. Pulicharla, S.K. Brar, Environ. Pollut. **267**, 115370 (2020)
5. M. Ángel Arguello-Pérez, J.A. Mendoza-Pérez, A. Tintos-Gómez, E. Ramírez-Ayala, E. Godínez-Domínguez, F.D.A. Silva-Bátiz, Water (Switzerland) (2019). https://doi.org/10.3390/w11071386
6. J. Siemens, G. Huschek, C. Siebe, M. Kaupenjohann, Water Res. **42**, 2124 (2008)
7. M.J. Ahmed, J. Environ. Manage. **190**, 274 (2017)
8. S. Chopra, D. Kumar, Heliyon **6**, e04087 (2020)
9. N. Taoufik, W. Boumya, M. Achak, M. Sillanpää, N. Barka, J. Environ. Manag. (2021). https://doi.org/10.1016/j.jenvman.2021.112404
10. K. Dhangar, M. Kumar, Sci. Total Environ. **738**, 140320 (2020)
11. M.J. Ahmed, B.H. Hameed, Ecotoxicol. Environ. Saf. **149**, 257 (2018)
12. C.P. Silva, G. Jaria, M. Otero, V.I. Esteves, V. Calisto, Biores. Technol. **250**, 888 (2018)
13. K. Okiel, M. El-Sayed, M.Y. El-Kady, Egypt. J. Pet. **20**, 9 (2011)
14. H.B. Quesada, A.T.A. Baptista, L.F. Cusioli, D. Seibert, C. De Oliveira Bezerra, R. Bergamasco, Chemosphere **222**, 766 (2019)
15. J. Ouyang, L. Zhou, Z. Liu, J.Y.Y. Heng, W. Chen, Sep. Purif. Technol. **253**, 117536 (2020)
16. C. Nieto Delgado and J. R. Rangel Mendez, *Preparation of Carbon Materials from Lignocellulosic Biomass* (2014), pp. 35–63
17. C.T. Brett, Int. Rev. Cytol. **199**, 161 (2000)
18. J.M. Dias, M.C.M. Alvim-Ferraz, M.F. Almeida, J. Rivera-Utrilla, M. Sánchez-Polo, J. Environ. Manage. **85**, 833 (2007)
19. D. Mohan, C.U. Pittman, P.H. Steele, Energy Fuels **20**, 848 (2006)
20. F. Rodríguez-Reinoso, M. Molina-Sabio, M.T. González, Carbon **33**, 15 (1995)
21. P. Samaras, E. Diamadopoulos, G.P. Sakellaropoulos, Carbon **32**, 771 (1994)
22. A.A. Peterson, F. Vogel, R.P. Lachance, M. Fröling, M.J. Antal, J.W. Tester, Energy Environ. Sci. **1**, 32 (2008)
23. M.M. Titirici, A. Thomas, S.H. Yu, J.O. Müller, M. Antonietti, Chem. Mater. **19**, 4205 (2007)
24. A. Funke, F. Ziegler, Biofuels Bioprod. Biorefining **4**, 160 (2010)
25. T.A. Khan, A.S. Saud, S.S. Jamari, M.H.A. Rahim, J.W. Park, H.J. Kim, Biomass Bioenergy (2019). https://doi.org/10.1016/j.biombioe.2019.105384
26. J.M.V. Nabais, M.M.P. Carrot, M.M.L. Ribeiro Carrot, J.A. Menéndez, Carbon **42**, 1315 (2004)
27. D.A. Jones, T.P. Lelyveld, S.D. Mavrofidis, S.W. Kingman, N.J. Miles, Resour. Conserv. Recycl. **34**, 75 (2002)
28. E. Ma, Q. Cervera, G.M. Mejía Sánchez, Bioresour. Technol. **44**, 61 (1993)
29. H. Li, Z. Sun, L. Zhang, Y. Tian, G. Cui, S. Yan, Colloids Surf., A **489**, 191 (2016)
30. D. Prahas, Y. Kartika, N. Indraswati, S. Ismadji, Chem. Eng. J. **140**, 32 (2008)
31. M.E. Fernandez, G.V. Nunell, P.R. Bonelli, A.L. Cukierman, Ind. Crops Prod. **62**, 437 (2014)

32. A. Reffas, V. Bernardet, B. David, L. Reinert, M.B. Lehocine, M. Dubois, N. Batisse, L. Duclaux, J. Hazard. Mater. **175**, 779 (2010)
33. S.M. Lamine, C. Ridha, H.M. Mahfoud, C. Mouad, B. Lotfi, A.H. Al-Dujaili, Energy Procedia **50**, 393 (2014)
34. F. Boudrahem, F. Aissani-Benissad, A. Soualah, J. Chem. Eng. Data **56**, 1804 (2011)
35. M.C. Baquero, L. Giraldo, J.C. Moreno, F. Suárez-García, A. Martínez-Alonso, J.M.D. Tascón, J. Anal. Appl. Pyrol. **70**, 779 (2003)
36. I. Robles, F. Espejel-Ayala, G. Velasco, A. Cárdenas, and L. A. Godínez, Biomass Convers. Biorefinery (2020)
37. P. Húmpola, H. Odetti, J.C. Moreno-Piraján, L. Giraldo, Adsorption **22**, 23 (2016)
38. A.K. Tovar, L.A. Godínez, F. Espejel, R.M. Ramírez-Zamora, I. Robles, Waste Manage. **85**, 202 (2019)
39. A. El Nemr, O. Abdelwahab, A. El-Sikaily, A. Khaled, J. Hazard. Mater. **161**, 102 (2009)
40. A. Khaled, A. El Nemr, A. El-Sikaily, O. Abdelwahab, J. Hazard. Mater. **165**, 100 (2009)
41. A. Khaled, A. El Nemr, A. El-Sikaily, O. Abdelwahab, Desalination **238**, 210 (2009)
42. S. Larous, A.H. Meniai, Int. J. Hydrogen Energy **41**, 10380 (2016)
43. M.D.G. de Luna, W. Budianta, K.K.P. Rivera, R.O. Arazo, J. Environ. Chem. Eng. **5**, 1465 (2017)
44. M. Malhotra, S. Suresh, A. Garg, Environ. Sci. Pollut. Res. **25**, 32210 (2018)
45. H. Nourmoradi, K.F. Moghadam, A. Jafari, B. Kamarehie, J. Environ. Chem. Eng. **6**, 6807 (2018)
46. S.N. Nandeshwar, A.S. Mahakalakar, R.R. Gupta, G.Z. Kyzas, J. Mol. Liq. **216**, 688 (2016)
47. S.D. Ashtaputrey, P.D. Ashtaputrey, J. Adv. Chem. Sci. **2**, 360 (2016)
48. S.A. Mirzaee, B. Bayati, M.R. Valizadeh, H.T. Gomes, Z. Noorimotlagh, Chem. Eng. Res. Des. **167**, 116 (2021)
49. M.J.B. Evans, E. Halliop, J.A.F. MacDonald, Carbon **37**, 269 (1999)
50. J.C. Moreno-Piraján, L. Giraldo, E-J. Chem. **9**, 926 (2012)
51. S. N. F. Ali, E. I. El-Shafey, S. Al-Busafi, and H. A. J. Al-Lawati, J. Environ. Chem. Eng. **7**, (2019)
52. M.F. Taha, M.H.C. Ibrahim, M.S. Shaharun, F.K. Chong, AIP Conf. Proc. **1482**, 252 (2012)
53. M. Bernardo, S. Rodrigues, N. Lapa, I. Matos, F. Lemos, M.K.S. Batista, A.P. Carvalho, I. Fonseca, Int. J. Environ. Sci. Technol. **13**, 1989 (2016)
54. K. Kante, C. Nieto-Delgado, J.R. Rangel-Mendez, T.J. Bandosz, J. Hazard. Mater. **201–202**, 141 (2012)
55. A.O. Abo El Naga, M. El Saied, S.A. Shaban, F.Y. El Kady, J. Mol. Liq. **285**, 9 (2019)
56. F. Boudrahem, F. Aissani-Benissad, H. Aït-Amar, J. Environ. Manage. **90**, 3031 (2009)
57. L.S. Oliveira, A.S. Franca, T.M. Alves, S.D.F. Rocha, J. Hazard. Mater. **155**, 507 (2008)
58. M. Gonçalves, M.C. Guerreiro, P.H. Ramos, L.C.A. De Oliveira, K. Sapag, Water Sci. Technol. **68**, 1085 (2013)
59. N.F.G.M. Cimirro, E.C. Lima, M.R. Cunha, S.L.P. Dias, P.S. Thue, A.C. Mazzocato, G.L. Dotto, M.A. Gelesky, F.A. Pavan, Environ. Sci. Pollut. Res. **27**, 21442 (2020)
60. A.B. Leite, C. Saucier, E.C. Lima, G.S. dos Reis, C.S. Umpierres, B.L. Mello, M. Shirmardi, S.L.P. Dias, C.H. Sampaio, Environ. Sci. Pollut. Res. **25**, 7647 (2018)
61. Y. Lv, L. Gan, M. Liu, W. Xiong, Z. Xu, D. Zhu, D.S. Wright, J. Power Sources **209**, 152 (2012)
62. S. Hashemian, K. Salari, Z.A. Yazdi, J. Ind. Eng. Chem. **20**, 1892 (2014)
63. L. Lonappan, T. Rouissi, R.K. Das, S.K. Brar, A.A. Ramirez, M. Verma, R.Y. Surampalli, J.R. Valero, Waste Manage. **49**, 537 (2016)
64. R. Ocampo-Perez, E. Padilla-Ortega, N.A. Medellin-Castillo, P. Coronado-Oyarvide, C.G. Aguilar-Madera, S.J. Segovia-Sandoval, R. Flores-Ramírez, A. Parra-Marfil, Sci. Total Environ. **655**, 1397 (2019)
65. P. Chakraborty, S.D. Singh, I. Gorai, D. Singh, W.U. Rahman, G. Halder, J. Water Process Eng. **33**, 101022 (2020)
66. K. Aydincak, T. Yumak, A. Sinağ, B. Esen, Ind. Eng. Chem. Res. **51**, 9145 (2012)
67. Y. Lei, H. Su, R. Tian, RSC Adv. **6**, 107829 (2016)
68. S. Başakçılardan Kabakcı, S.S. Baran, Waste Manag. **100**, 259 (2019)
69. D. Zhou, D. Li, A. Li, M. Qi, D. Cui, H. Wang, H. Wei, J. Environ. Chem. Eng. (2021). https://doi.org/10.1016/j.jece.2020.104671
70. R.A. Canales-Flores, F. Prieto-García, Diam. Relat. Mater. (2020). https://doi.org/10.1016/j.diamond.2020.108027
71. S. Salem, Z. Teimouri, A. Salem, Adv. Powder Technol. **31**, 4301 (2020)
72. G. Kaur, N. Singh, A. Rajor, Environ. Technol. Innov. **23**, 101601 (2021)
73. Y.S. Ho, J.C.Y. Ng, G. McKay, Sep. Purif. Methods **29**, 189 (2000)
74. V. L. Snoeyink and R. S. Summers, in *Water Quality and Treatment: A Handbook of Community Water Supplies*, edited by Letterman. R. D. (McGraw Hill, New York, USA, 1999), pp. 670–671
75. J.C.M. Weber, J. Walter, J. Sanit. Eng. Div. **89**, 31 (1963)
76. M. Benjelloun, Y. Miyah, G. Akdemir Evrendilek, F. Zerrouq, S. Lairini, Arab. J. Chem. **14**, 103031 (2021)
77. C. Martínez-Sánchez, L.M. Torres-Rodríguez, R.F.G. De La Cruz, Quim. Nova (2013). https://doi.org/10.1590/S0100-40422013000800022
78. K.S. Bharathi, S.T. Ramesh, Appl Water Sci **3**, 773 (2013)
79. C. Martínez-Sánchez, L. M. Torres-Rodríguez, and R. F. García-de La Cruz, J. Braz. Chem. Soc. **27**, (2016)
80. C. Martínez-Sánchez, L.M. Torres-Rodríguez, L.H. Velázquez-Jiménez, J.I. Sustaita-Martínez, R.F. García-delaCruz, Electroanalysis (2012). https://doi.org/10.1002/elan.201200052
81. A. Yazidi, L. Sellaoui, G.L. Dotto, A. Bonilla-Petriciolet, A.C. Fröhlich, and A. Ben Lamine. J. Mol. Liq. **283**, 276 (2019)
82. H.A. Al-Yousef, B.M. Alotaibi, M.M. Alanazi, F. Aouaini, L. Sellaoui, A. Bonilla-Petriciolet, J. Environ. Chem. Eng. **9**, 104950 (2021)
83. S.N. Oba, J.O. Ighalo, C.O. Aniagor, C.A. Igwegbe, Sci. Total Environ. **780**, 146608 (2021)
84. R.M. de Souza, H.B. Quesada, L.F. Cusioli, M.R. Fagundes-Klen, R. Bergamasco, Ind. Crops Prod. (2021). https://doi.org/10.1016/j.indcrop.2020.113200
85. V.T. Nguyen, T.M.T. Nguyen, Y.G. Liu, Q.Y. Cai, Environ. Eng. Sci. **38**, 974 (2021)
86. Y. M. Correa-Navarro, J. C. Moreno-Piraján, and L. Giraldo, Braz. J. Chem. Eng. (2021)
87. N. T. M. Tam, Y. G. Liu, H. Bashir, P. Zhang, S. B. Liu, X. Tan, M. Y. Dai, and M. F. Li, Front. Chem. **8**, (2020)
88. A.C. Fröhlich, R. Ocampo-Pérez, V. Diaz-Blancas, N.P.G. Salau, G.L. Dotto, Chem. Eng. J. **341**, 65 (2018)
89. A.C. Fröhlich, G.S. dos Reis, F.A. Pavan, É.C. Lima, E.L. Foletto, G.L. Dotto, Environ. Sci. Pollut. Res. **25**, 24713 (2018)
90. A.F.M. Streit, G.C. Collazzo, S.P. Druzian, R.S. Verdi, E.L. Foletto, L.F.S. Oliveira, G.L. Dotto, Chemosphere (2021). https://doi.org/10.1016/j.chemosphere.2020.128322

91. M.O. Omorogie, J.O. Babalola, M.O. Ismaeel, J.D. McGettrick, T.M. Watson, D.M. Dawson, M. Carta, M.F. Kuehnel, Adv. Powder Technol. **32**, 866 (2021)
92. N.A. Salem, S.M. Yakoot, Int. J. Pharmacol. **12**, 729 (2016)
93. S. Show, B. Karmakar, and G. Halder, Biomass Conver. Biorefinery (2020)
94. S. Mondal, S. Patel, S.K. Majumder, Water Air Soil Pollut. (2020). https://doi.org/10.1007/s11270-020-4411-7
95. R.A. Reza, M. Ahmaruzzaman, Res. Chem. Intermed. **42**, 1463 (2016)
96. F. Tomul, Y. Arslan, B. Kabak, D. Trak, E. Kendüzler, E.C. Lima, H.N. Tran, Sci. Total Environ. (2020). https://doi.org/10.1016/j.scitotenv.2020.137828
97. H.A. Al-Yousef, B.M. Alotaibi, F. Aouaini, L. Sellaoui, A. Bonilla-Petriciolet, J. Mol. Liq. (2021). https://doi.org/10.1016/j.molliq.2021.115697
98. A. Gómez-Avilés, L. Sellaoui, M. Badawi, A. Bonilla-Petriciolet, J. Bedia, C. Belver, Chem. Eng. J. (2021). https://doi.org/10.1016/j.cej.2020.126601
99. J. Shin, J. Kwak, Y.G. Lee, S. Kim, M. Choi, S. Bae, S.H. Lee, Y. Park, K. Chon, Environ. Pollut. **270**, 116244 (2021)
100. J.J. Rueda-Márquez, J. Moreno-Andrés, A. Rey, C. Corada-Fernández, A. Mikola, M.A. Manzano, I. Levchuk, Water Res. (2021). https://doi.org/10.1016/j.watres.2021.116833
101. A.C. Sophia, E.C. Lima, Ecotoxicol. Environ. Saf. **150**, 1 (2018)
102. A. Rao, A. Kumar, R. Dhodapkar, and S. Pal, Environ. Sci. Pollut. Res. (2021)
103. M. Varga, M. ELAbadsa, E. Tatár, V.G. Mihucz, Microchem. J. **148**, 661 (2019)
104. H.E. Reynel-Avila, D.I. Mendoza-Castillo, A. Bonilla-Petriciolet, J. Silvestre-Albero, J. Mol. Liq. **209**, 187 (2015)
105. J.L. Sotelo, A. Rodríguez, S. Álvarez, J. García, Chem. Eng. Res. Des. **90**, 967 (2012)
106. A. Mokhati, O. Benturki, M. Bernardo, Z. Kecira, I. Matos, N. Lapa, M. Ventura, O.S.G.P. Soares, A.M.B. Do Rego, I.M. Fonseca, J. Mol. Liq. **326**, 115368 (2021)
107. W. Sun, H. Li, H. Li, S. Li, X. Cao, Chem. Eng. J. **360**, 645 (2019)
108. S. Álvarez-Torrellas, M. Muñoz, J.A. Zazo, J.A. Casas, J. García, J. Environ. Manage. **183**, 294 (2016)
109. N. Cheng, B. Wang, P. Wu, X. Lee, Y. Xing, M. Chen, B. Gao, Environ. Pollut. **273**, 116448 (2021)
110. C. Silveira, Q.L. Shimabuku-Biadola, M.F. Silva, M.F. Vieira, R. Bergamasco, Environ. Sci. Pollut. Res. **27**, 6088 (2020)
111. Z. Shirani, H. Song, A. Bhatnagar, Sci. Total Environ. **745**, 140789 (2020)
112. C. Jung, L.K. Boateng, J.R.V. Flora, J. Oh, M.C. Braswell, A. Son, Y. Yoon, Chem. Eng. J. **264**, 1 (2015)
113. P.V. Viotti, W.M. Moreira, O.A.A. dos Santos, R. Bergamasco, A.M.S. Vieira, M.F. Vieira, J. Clean. Prod. **219**, 809 (2019)
114. M.A.E. de Franco, C.B. de Carvalho, M.M. Bonetto, R. de Pelegrini Soares, L.A. Féris, J. Clean. Prod. **181**, 145 (2018)
115. L.A. Araujo, C.O. Bezerra, L.F. Cusioli, M.F. Silva, L. Nishi, R.G. Gomes, R. Bergamasco, J. Environ. Chem. Eng. **6**, 7192 (2018)
116. C. Saucier, M.A. Adebayo, E.C. Lima, R. Cataluña, P.S. Thue, L.D.T. Prola, M.J. Puchana-Rosero, F.M. Machado, F.A. Pavan, G.L. Dotto, J. Hazard. Mater. **289**, 18 (2015)
117. M. Grassi, G. Kaykioglu, V. Belgiorno, and G. Lofrano, in *SpringerBriefs in Green Chemistry for Sustainability* (2012), pp. 15–37
118. M. Sulyman, J. Namiesnik, A. Gierak, Pol. J. Environ. Stud. **26**, 479 (2017)
119. G.Z. Kyzas, A.C. Mitropoulos, Proceedings **2**, 652 (2018)
120. L. Nielsen, T.J. Bandosz, Microporous Mesoporous Mater. **220**, 58 (2016)
121. M. León, J. Silva, S. Carrasco, N. Barrientos, Processes (2020). https://doi.org/10.3390/pr8080945
122. M. Ahmaruzzaman, Adv. Coll. Interface. Sci. **143**, 48 (2008)
123. S. Chowdhury, J. Sikder, T. Mandal, G. Halder, Sci. Total Environ. **665**, 438 (2019)
124. P. Chakraborty, S. Banerjee, S. Kumar, S. Sadhukhan, G. Halder, Process Saf. Environ. Prot. **118**, 10 (2018)